13th International Conference on
Structural Health Monitoring of Intelligent Infrastructure
DOI: 10.3217/978-3-99161-057-1-008

Updating prediction of fatigue reliability index of railway bridges using structural monitoring data and updated load histories

Marian Ralbovsky[1, ORCID 0000-0001-9323-4508], Stefan Lachinger[1, ORCID 0009-0005-6705-6118]
[1]Center for Transport Technologies, Austrian Institute of Technology GmbH, Giefinggasse 4, 1210 Wien, Austria
email: marian.ralbovsky@ait.ac.at, stefan.lachinger@ait.ac.at

ABSTRACT: The assessment of fatigue consumption and the remaining lifetime of structural components is affected by considerable uncertainties on the side of the traffic loads, fatigue resistance and structural response. The purpose of the presented work was to develop methods for dealing with these uncertainties, as well as methods for improving the accuracy of assessment with the use of additional data.
Within the research project Assets4Rail, a structural monitoring system was installed on a railway bridge located on a local track in Austria. The system consisted of strain sensors, acceleration sensors and inclinometers. It was used to measure the bridge response during train passages with known axle loads in course of a test with controlled conditions. This data was used to calibrate the structural model and develop probabilistic methods for fatigue assessment. Influence lines at fatigue-critical locations were evaluated from measured bridge strain response including their uncertainty. Further uncertainties considered in the assessment include the load histories and the fatigue resistance.
The results showed the largest contribution by evaluation of model uncertainties from monitoring data. The effect of model updating was also considerable, but less significant. Further increase of estimation accuracy is achieved using section-specific traffic data. Whereas wayside monitoring data represent the reference scenario, the use of traffic management data provides a usable alternative.

KEY WORDS: fatigue; probabilistic; reliability; monitoring; updating.

1 INTRODUCTION

Railway bridges are often designed in steel. Their high ratio of traffic load to dead load as well as the high train axle forces makes them prone to fatigue issues. Many structures or components are reaching their planned lifetime. A survey conducted by the European project Sustainable Bridges, revealed that 75% of steel railway bridges are over 50 years old and almost 35% of them are over 100 years old [1]. Although fatigue damage is not among the leading causes of bridge collapses [2], it plays a role in maintenance of railway infrastructure. To optimize the investment planning for railway bridge maintenance and replacement, it is therefore advantageous to perform more accurate assessment of their expected remaining fatigue lifetime.

Several techniques to this end have already been developed and tested. The application of monitoring techniques to capture the real structural behavior has been implemented in many variants, usually evaluating the stress spectra from strain data acquired at fatigue-critical locations and consequent application of the Miner's rule to determine the damage accumulation [3]. The use of monitoring data leads often to lower stress ranges compared to results predicted by numerical models due to their inherent simplifications and their aspiration to ensure sufficient structural safety. Thus, SHM-based evaluations tend to predict a more extended fatigue lifetime. However, some application cases [4] show that it is not to be generalized as a rule.

Through a combination of monitoring data with calibrated FE-models, stress spectra can be evaluated also at unmeasured locations. This technique of virtual sensing has been validated [5], [6] to obtain nominal stresses at railway bridges equipped with strain and acceleration sensors. The modelling can be further extended using the multiscale approach to also evaluate the local stresses – for example using a 3-scale concept encompassing the global scale, the structural member scale and the local scale [7].

Besides monitoring the structural response, the estimation of overpassing axle-load histories is the next important parameter in the fatigue accumulation assessment. While the train mixes defined in the Eurocode are suitable for design of new bridges, for the assessment of existing structures it is more expedient to use axle-load histories specific to the respective track location. The actual axle loads can be acquired for example using wayside monitoring systems applied on rails. However, the application of such systems is relatively new, so they provide data on the current state of traffic loading and axle-load histories prior to their installation remain unmeasured. During bridge lifetime, the axle-load histories may have changed significantly. Reconstruction of historic traffic loads provides a possible solution, as shown in a study for Norwegian railway bridges [8]. In here, it was identified that modern freight trains introduced after 1985 increased the fatigue damage accumulation rate significantly. Based on axle-load measurements in Dutch railway network, new fatigue load models for bridge assessment were proposed [9]. One of the load models addresses the period before 1970 and is based on limited available data and expert judgement. In another study [10], a simple approach was proposed, which considers development of total rail traffic volumes on national level, but neglects changes in train composition over time.

CC BY 4.0
https://creativecommons.org/licenses/by/4.0/deed.en
This CC license does not apply to third party material and content noted otherwise

DOI: 10.3217/978-3-99161-057-1-008

The evaluation of remaining fatigue lifetime is typically based on S-N curves as the definition of material resistance to fatigue loads. This approach features a fair amount of conservatism [11], which is understandable considering the significant variance of fatigue test results and the requirements of structural reliability, and it is necessary in semi-probabilistic assessment. However, the uncertainties can be modeled using a full-probabilistic approach by formulating the fatigue resistance as a random variable and evaluating probabilities of its exceedance. This type of evaluation results in estimating the reliability index and its development as the fatigue damage accumulates over time [12].

This work, which was done within the Shift2Rail project Assets4Rail [13], combines several abovementioned aspects, with the aim to highlight the joined effect of several methods. Three areas of more accurate fatigue assessment are addressed here: monitoring of structural response, track-specific axle-load histories, and probabilistic modelling of fatigue resistance. Moreover, the issue of track-specific axle-load histories is handled in different cases of data availability.

2 STRUCTURAL MONITORING AND MODEL CALIBRATION

2.1 Bridge description

The bridge is a semi-through type truss steel bridge (U-frame), which was constructed in the 1990's (Figure 1). It is a single span of 41.67 m length, which consists of 10 segments of equal length. The top chord has a rectangular cross-section, while the bottom chord is U-shaped. The diagonals have I-shaped cross section, except for the outer diagonals with rectangular cross-section. The truss members are constructed from welded steel plates and the truss members connect to each other with bolted plates.

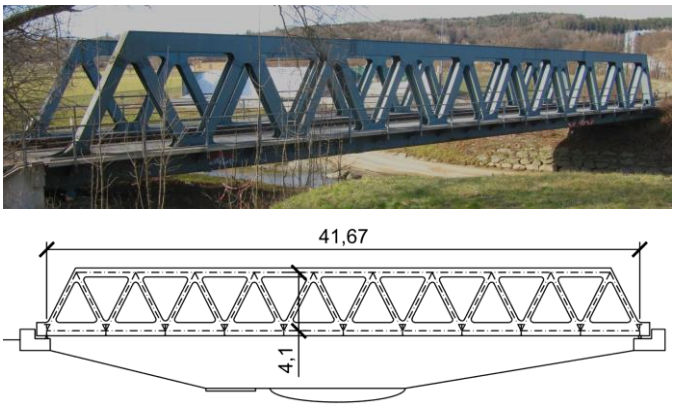

Figure 1. Side view of the bridge.

The bridge carries a single unballasted railway track. The rails are placed on top of wooden sleepers carried by longitudinal beams, which are rigidly connected to transverse beams (Figure 2). The transverse beams connect to bottom chord of the truss. The connections are again executed using bolted plates. The bridge deck has two layers of diagonal bracing, stiffening the longitudinal beams under the sleepers, as well as bottom chords of the truss.

Figure 2. Structure of the bridge deck.

The bridge is located on a side track in Austrian railway network and experiences very low traffic volumes. This facilitated performing various tests and measurements on this bridge. For purposes of this study, a traffic constitution was assumed with properties that correspond to a main railway line, thus simulating high traffic volumes.

2.2 Measurement system

The bridge was equipped with 31 optical strain gauges. The sensor locations concentrated around truss-member connections between truss segments 4 and 5 (Figure 3), as well as connection between longitudinal and transverse beams at segment 8 and the transverse beam to truss chord connection (Figure 4). Since the fatigue evaluation was indented to be based on nominal stresses, the purpose of this monitoring system was to capture nominal stresses in structural members, which explains positioning the sensors at a little distance from the connection nodes and not directly on the fatigue hot spots.

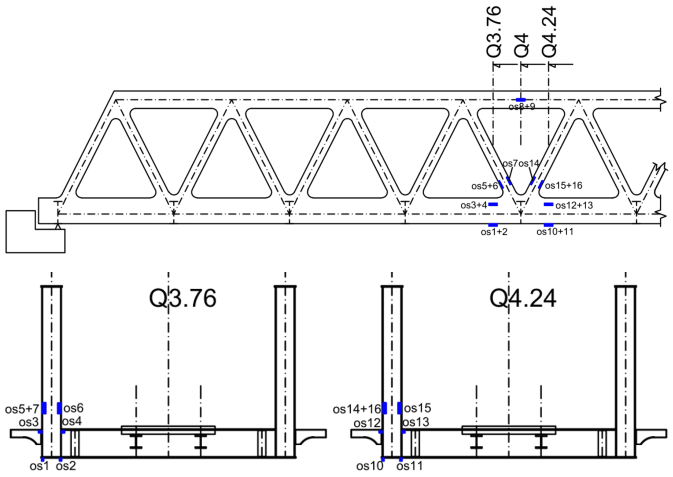

Figure 3. Locations of fibre-optic strain sensors on truss members.

The sensors were located on several points of the same cross-section to increase accuracy of the measurement and also to capture secondary effects like transverse bending or warping of cross-sections. Additionally, acceleration sensors were placed on several locations across the bridge, as well as inclinometers and temperature sensors. However, they are not relevant for the purposes of the work presented here, therefore they will not be described here.

CC BY 4.0
https://creativecommons.org/licenses/by/4.0/deed.en
This CC license does not apply to third party material and content noted otherwise

DOI: 10.3217/978-3-99161-057-1-008

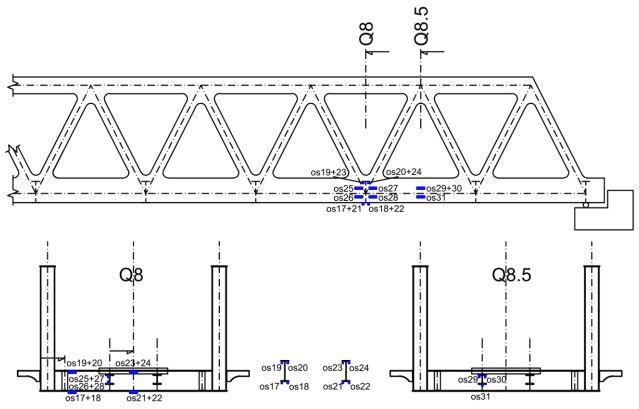

Figure 4. Locations of fibre-optic strain sensors on transverse and longitudinal beams.

The Bragg grating of the fibre-optic strain sensors provides an active sensor length of 10 cm. The actual sensor is held by threaded extension rods, which increase the effective measurement length to 50 cm in total. This enables a higher sensitivity of the sensor, which was required to capture the relatively low strains. The extension rods are connected to the structure through strong magnets. In this way, the layers of corrosion protection remained untouched in spite of sensor application. However, such mounting of the sensors (Figure 5) causes also an offset between the structure's surface and the sensor axis. This means that the strain captured by the sensor is not the same as the strain at the structure surface, if the cross-section experiences bending moments. Since several sensors were installed in each cross-section, the measured strains can be interpolated to any other (unmeasured) point of the cross-section, assuming linear strain gradients within a cross-section.

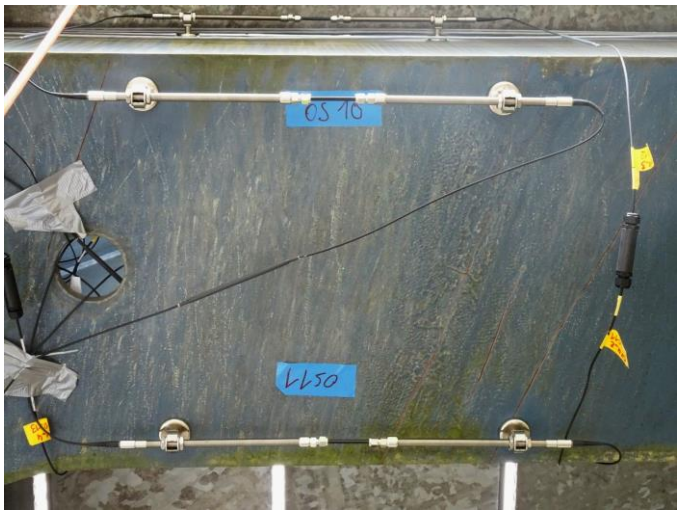

Figure 5. Fibre-optic strain sensors mounted using magnets and threaded extension rods.

The strains were measured during passages of a test train, which consisted of a diesel-powered locomotive with 32 t weight on two axles, followed by two 4-axle wagons weighing 78.4 t and 49.45 t, respectively, and one 2-axle wagon weighing 18 t. The train passages were repeated with different speeds ranging from 5 to 40 km/h, reaching ca. 100 passages in total.

In order to relate axle loads to the measured strain response, it is expedient to transform the measured strain signals from the time domain to the domain of axle positions. This was done by identification of axle positions in the measured strain signals, and transforming the time to the distance covered by the first train axle, starting at the bridge abutment above the bearing.

The differences between strain signals measured during different passages of the test train were relatively small. They are displayed in Figure 6 for two selected sensors. The top figure shows results from sensor OS10 located at the bottom chord of the truss, while the bottom figure shows results from sensor OS21 located in midspan of the transverse beam. Records of individual train passages are displayed as thin grey lines, and their mean is displayed as bold blue line.

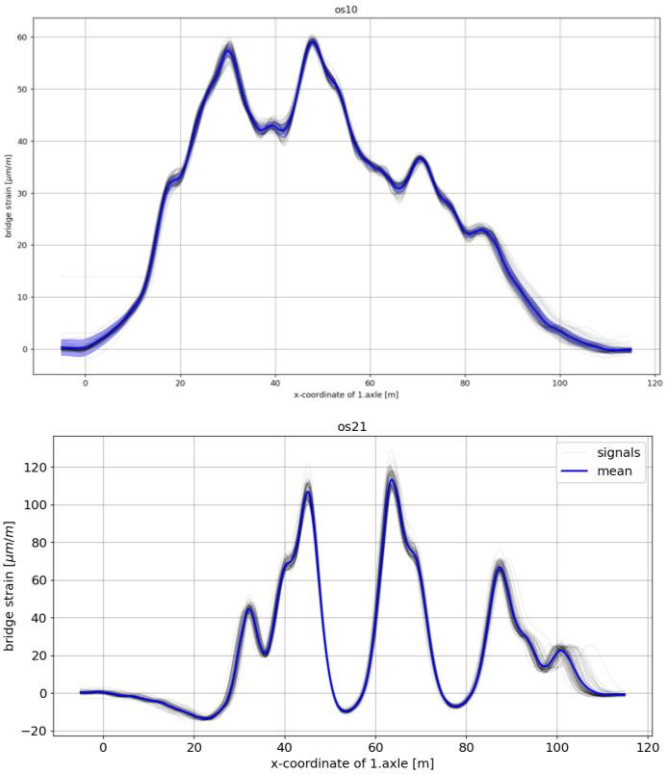

Figure 6. Strains during 102 passages of the test train measured at the bottom chord (top) and at the transverse beam (bottom).

The measured responses were used to calibrate the numerical model that was later used for estimation of fatigue damage accumulation.

Additionally to the static structural response, dynamic resonance parameters were identified from acceleration measurements, and used in calibration of the numerical model. Three identified modes were used to this end; their frequencies are listed in Table 1. The first was a global mode of vertical bending with one half-wave along the span length. The other two modes represent lateral vibration of the upper chord, with 1 and 1.5 waves along the span length, respectively. The agreement between frequencies of the numerical model and the ones identified from measurements were good already for the initial model, indicating its high quality.

CC BY 4.0
https://creativecommons.org/licenses/by/4.0/deed.en
This CC license does not apply to third party material and content noted otherwise

DOI: 10.3217/978-3-99161-057-1-008

Table 1. Comparison of measured eigenfrequencies with predictions of the initial numerical model.

Parameter	Measured	FE-Model
f_1, vertical bending	5.40 Hz	5.48 Hz
f_2, upper chord 1 wave	9.99 Hz	10.22 Hz
f_3, upper chord 1.5 waves	12.19 Hz	13.04 Hz

2.3 Model calibration

The numerical analysis was done using a shell model, which was constructed, meshed and calculated using FOSS (Free and Open Source Software) products. In particular the Pre- and Post-Processing platform SALOME [14] was used for the geometrical construction and meshing of the model, while the FEM-Solver CalculiX [15] was used for solving the meshed model. The model optimization of the FE-model was conducted using self-made algorithms in the Python programming language, utilizing optimization routines of the SciPy (Scientific Python) package.

The symmetry of the structure as well as the loading was used to reduce the model size and work with only half of the bridge and respective symmetry conditions (Figure 7, top). As the analysis will be done on the level of nominal stresses, a detailed modelling of the bolted connections was not necessary; the connections were modeled as rigidly connected plates (Figure 7, bottom).

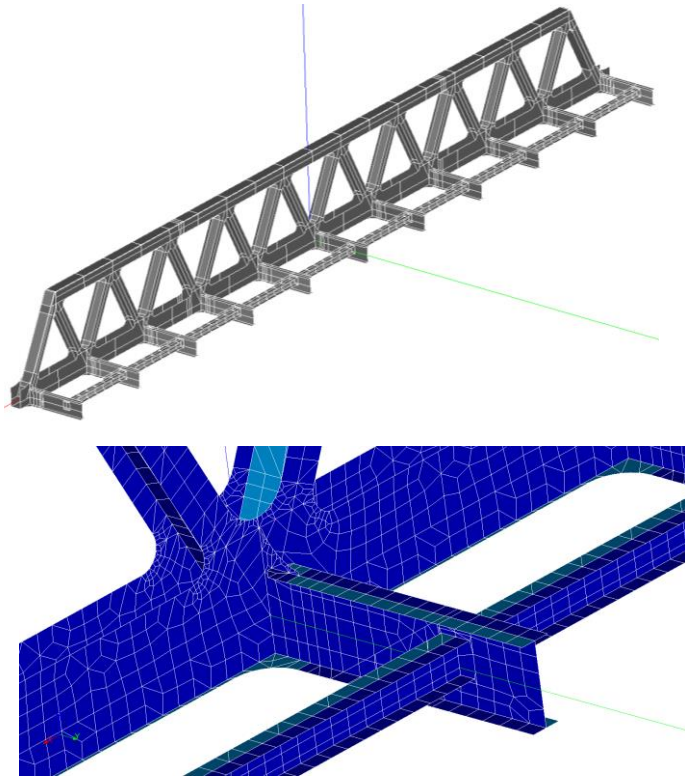

Figure 7. Geometry of the FE-model (top) and a detail of its mesh (bottom).

Using modal analysis of the bridge structure, several eigenfrequencies and mode shapes were calculated; the first two of which are displayed in Figure 8.

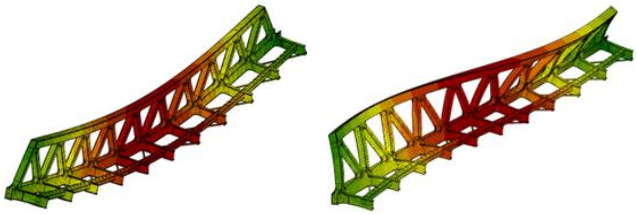

Figure 8. Mode shapes of the FE-model: f_1=5.48 Hz (left) and f_2=10.22 Hz (right).

The model calibration was performed in three steps: 1. using measured strain responses during train passages, 2. using measured eigenfrequencies and mode shapes, 3. using both sets of measured data together. The updating was done twice, using two different objective functions: the squared differences approach (Eq.1) and the Gauss error function approach (Eq.2).

$$J_{sq} = \sum_{i=1}^{m} \left(\frac{z_n(i) - z_e(i)}{\sigma_e(i)} \right)^2 \quad (1)$$

$$J_{erf} = \sum_{i=1}^{m} erf\left(w \cdot \frac{|z_n(i) - z_e(i)|}{\sigma_e(i)\sqrt{2}} \right) \quad (2)$$

The structural parameters that were subjected to updating are listed in Table 2. They comprise of relevant parameters affecting the global stiffness, stiffness of connections, as well as distribution of structural masses.

Table 2. Values of updating parameters.

Parameter	Initial value	Updated with J_{sq}	Updated with J_{erf}
Young's modulus [GPa]	210	220.5	205.8
Steel density [kg/m³]	7850	8282	8282
Coef. for cross-girder connection stiffness	1	1.5	1.31
Coef. for main truss connection stiffness	1	1.5	0.683
Translation rail spring [MN/m]	0	0	0
Rotational bearing spring [MNm/m]	0	1000	0
Coef. for sidewalk mass	1	1.1	0.9
Cover plate mass coef.	1	1.1	0.9
Thickness of stiffener at cross-girder connection [mm]	17.5	20.2	19.2

The two updating algorithms suggested different solutions for the updating parameters. While the squared differences approach favored increase of both stiffness (global and connections) and masses, the updating approach of Gauss error function suggested in comparison lower connection stiffness and non-structural masses. The agreement of the updated parameters with their real values could not be checked due to significant effort that would be required for such testing. This would be also the usual case in any other real applications.

The updated models were subsequently used in evaluation of fatigue damage evaluation at selected fatigue-critical details. Five critical details were identified in total. The first three of them are displayed in Figure 9. Most critical was detail nr.3, which covers fatigue failure in the lateral direction in the stiffener plate at the toe weld. The upper fillet weld produced a

CC BY 4.0
https://creativecommons.org/licenses/by/4.0/deed.en
This CC license does not apply to third party material and content noted otherwise

DOI: 10.3217/978-3-99161-057-1-008

detail category of 36 N/mm² for a root crack at the weld, which ranked it as most fatigue-critical spot on the structure.

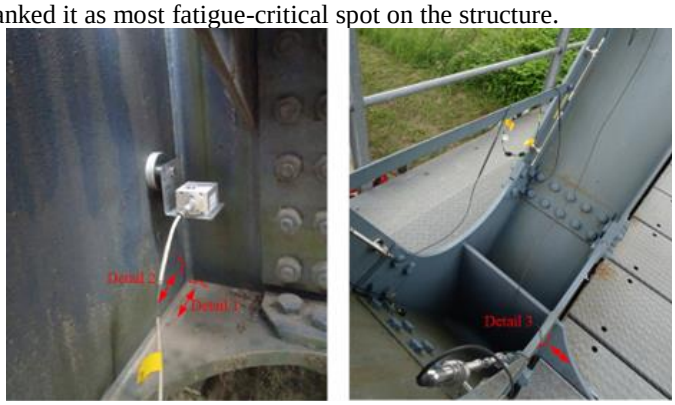

Figure 9. Three fatigue-critical details at the connection of cross-girder to bottom chord of the truss.

The differences in updated structural parameters resulted in influence lines of strain at fatigue-critical location as presented in Figure 10.

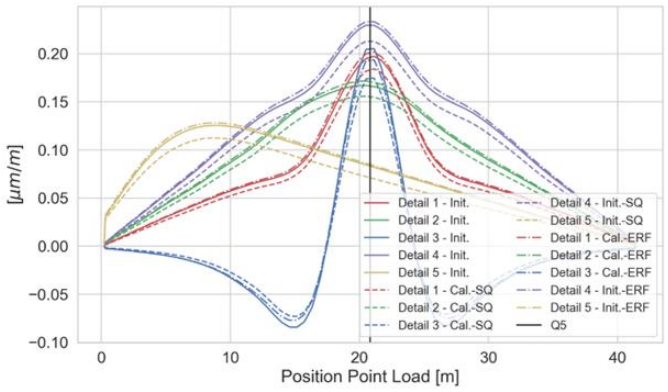

Figure 10. Influence lines of strain at five fatigue-critical details before updating (solid lines), after updating with… (dashed lines) and after updating with … (dash-dotted lines).

3 TRAFFIC LOADS

To highlight the difference of traffic load assumptions in different cases of data availability, three cases were considered:

- No track-specific data available
- Traffic management data available for given section
- Wayside monitoring data available for given section

The first case represents the usual situation used in design of new bridges, where the train mix according to Eurocode is used. In the second case, the traffic management data provide basic information about train traffic specific to the track section. This information includes total train length, total train weight (estimated from wagon specifications), number of wagons and type of locomotive, and is listed for all train passages in a given time period. The third case represents the most accurate information: data from a wayside monitoring system, which provide axle forces and axle spacings of all train passages in a given time period.

Since the availability of wayside monitoring data is generally limited, it is expedient to have a methodology that can use traffic management data to generate track-specific estimation of traffic loads. Such a methodology was developed within the Assets4Rail project. Detailed description of the methodology can be found in [16]; in this paper only a brief outline can be presented.

The procedure evaluates basic properties of trains from train management data and groups similar trains into clusters. For freight trains, the chosen basic properties were: unit mass of wagons [t/m], unit mass of locomotive(s) [t/m], and the number of carriages. Clustering algorithms were used to create train groups from available data, and then evaluate statistical properties of each group created. Figure 11 shows an example of evaluated train groups, represented by individual boxes. The placing and dimension of the displayed boxes correspond to the range $\langle \pi - \sigma; \mu + \sigma \rangle$ of the three parameters annotated on the respective axes. The number in center of each box indicated the cluster size, i.e. number of train passages that were grouped in the respective cluster.

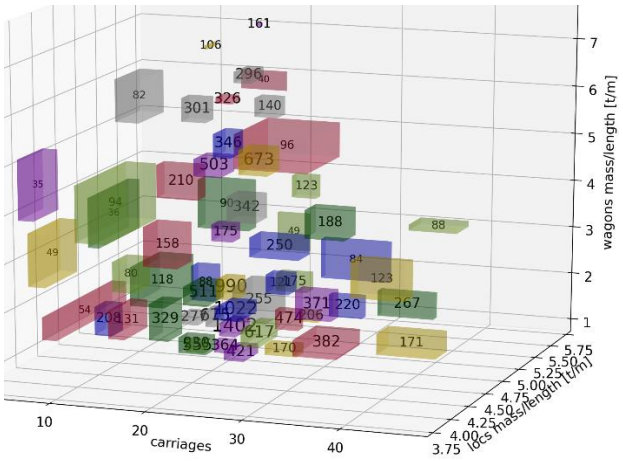

Figure 11. Clustered train management data of freight trains.

In the next step, a representative axle sequence was generated for each cluster. A database of wagon properties and a train model generation algorithm developed within the Assets4Rail project was used to this end. This algorithm requires deterministic values of basic train properties (number of carriages, etc.) as input: one set of values for each cluster. From the statistical evaluation of train data within each cluster, different quantiles can be chosen to represent each cluster. In order to compare the differences, the quantiles of 25%, 50%, 75% and 95% were used in further evaluations.

Schemes of generated axle sequences for 10 selected clusters of freight trains is partly shown in Figure 12; they consist of a sequence of arrows, height of which is proportional to the axle force magnitude. Loading situation of individual wagons (empty / full) is considered.

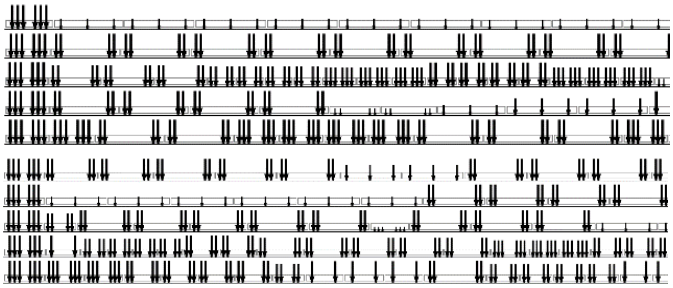

Figure 12. Partial schemes of freight train axle-sequences generated for selected train clusters.

CC BY 4.0
https://creativecommons.org/licenses/by/4.0/deed.en
This CC license does not apply to third party material and content noted otherwise

DOI: 10.3217/978-3-99161-057-1-008

In each train scheme, a locomotive with 6 axles is visible on the left side; the axle-force arrows display a force of 220 kN. The empty wagons can be recognized by the very small axle-forces shown at the wheel positions, which correspond to forces of less than 100 kN. The wagons feature different lengths (15 – 25 m) and axle configurations, which were chosen from catalogues of existing wagon stock.

Comparison of the track-specific train properties with the fatigue load model of the Eurocode showed some differences presented in Figure 13. The unit mass of the trains was considerably lower compared to the Eurocode standard traffic mix, while the number of axles was slightly higher in the freight trains. The shown results refer to one of the locations within Austrian railway network that was analyzed.

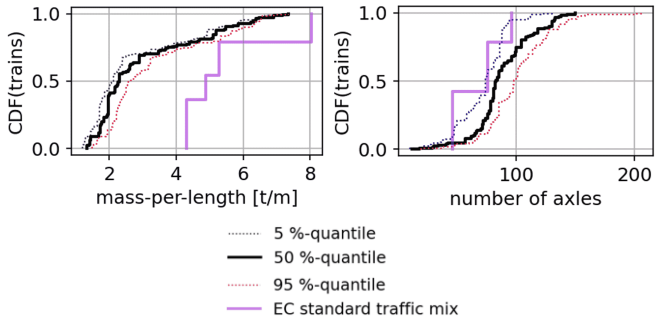

Figure 13. Cumulative Density Functions of the unit train mass (left) and number of axles (right) for trains generated from train management data compared to Eurocode.

In order to compare the differences between different axle-load sequences, their effect on the fatigue damage accumulation on different systems was analyzed. For this purpose, the midspan bending moment in simply-supported single-span bridges was used, simulating fatigue critical details governed by longitudinal stresses at such location. The span length was varied between 4 and 60 m. Eight traffic load mixes were analyzed: three Eurocode traffic mixes (light, standard, heavy), four traffic mixes generated the train management data using 25%, 50%, 75%, 95% quantiles of basic train properties for each cluster (TRGEN:_q25, _q50, _q75, _q95), and finally axle-sequences as measured by a wayside monitoring system. The fatigue damage accumulation evaluated using the wayside monitoring data was used as reference (d_{ref}), since it represents the most accurate result. To eliminate the influence of total traffic volume, all traffic mixes were normalized the total traffic volume of 25 Mt/year. Figure 14 shows a comparison of the evaluated fatigue damages in relation to the reference (wayside monitoring data).

This comparison shows that the Eurocode standard traffic mix produced a fatigue damage that exceeds the reference by 50% - 160%, depending on the span length. The dependance of this exceedance on the span length could be caused by the way the Eurocode models were calibrated, and may vary for bridges with different static systems.

Using the train management data, this conservativism would be reduced to 35% - 105% exceedance.

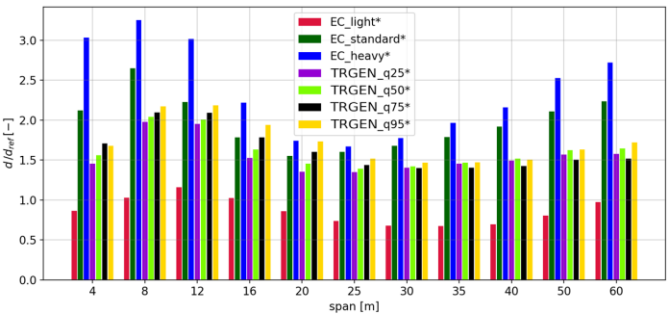

Figure 14. Fatigue damage accumulation evaluated for different normalized traffic mixes relative to d_{ref}.

4 FATIGUE RELIABILITY EVALUATION

A full-probabilistic approach was chosen to evaluate the reliability index of fatigue damage occurrence. This included probabilistic modelling of structural properties, traffic load actions, as well as the fatigue resistance. The distributions of many of the probabilistic variables were adopted based on the recommendations of the probabilistic model code [17]. The limit state function was defined according Eq. 3, where D_{cr} is the accumulated fatigue damage at the failure (defined as a probabilistic variable) and D_{Year} is the fatigue damage accumulation within one year (also a probabilistic variable).

$$G(t) = D_{cr} - D_{Year} \cdot t \tag{3}$$

The failure probability and the reliability index are then evaluated using Eq. 4 and 5, respectively.

$$P_f(t) = P[T \leq t] = P[G(t) < 0] \tag{4}$$

$$\beta = -\Phi^{-1}(P_f) \tag{5}$$

Figure 15 shows D_{Year} for the detail Nr. 3, compared between different models. The blue curve represents the case without using any monitoring data (no prior information) and results into the highest estimates of damage accumulation. If the model uncertainty can be estimated from the monitoring data, it can substantially reduce the total uncertainties. In here, the model uncertainty was determined from the uncertainty of influence lines evaluated from the measurements with the test train and the resulting distribution of damage accumulation (the orange curve) shows a significant reduction as result. The influence lines still correspond to the initial model, i.e. without updating.

After the model updating, the evaluated damage accumulation shows further reduction, as it can be observed from the green curve obtained using updating with the squared differences approach (Eq.1), and red curve obtained using updating with the Gauss error function approach (Eq.2).

CC BY 4.0
https://creativecommons.org/licenses/by/4.0/deed.en
This CC license does not apply to third party material and content noted otherwise

DOI: 10.3217/978-3-99161-057-1-008

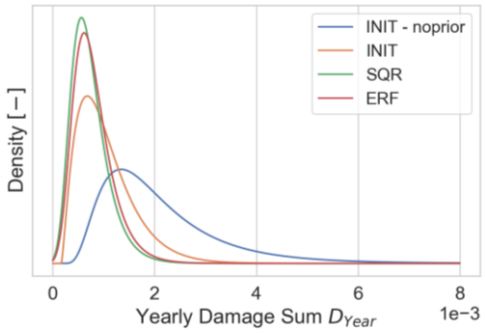

Figure 15. Distribution of the yearly fatigue damage accumulation on detail 3 using different numerical models.

The Figure 16 shows the reliability index evaluated at different points in time, comparing the same evaluation cases as in Figure 15: blue curve – without monitoring, orange curve – model uncertainty from monitoring but no updating, green and red curves – with additional model-updating step. The minimum required value of the reliability index is specified to be in range 1.5 – 3.8, depending on the accessibility of the detail and other factors. This range is displayed as a grey area. The failure probabilities related to reliability indices of β=1.5 and β=3.8 are P_f = 0.067 and P_f = 7.23 .10^{-5}, respectively.

Whereas without monitoring data, the reliability index would reach after 100 years the value of β=2.1 (P_f = 0.018), the inclusion of monitoring data combined with model updating could increase the reliability index value up to β=4.35 (P_f = 6.8 .10^{-6}) in this particular case.

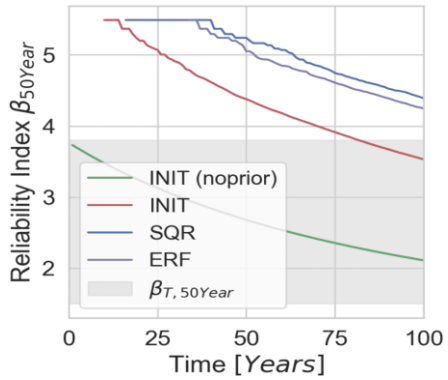

Figure 16. Development of the reliability index for detail 3 over time: comparison of different models.

5 CONCLUSIONS

The presented work summarizes the uncertainty parameters affecting fatigue damage evaluations and shows a way of dealing with them in a full-probabilistic analysis. The traffic loads can be updated using section-specific data, preferably wayside monitoring data that provide measured axle-load sequences. Alternatively, train management data can also be used to derive alternative, section-specific axle-sequences for fatigue evaluations. Since they rely on less accurate data regarding train masses compared to wayside monitoring, they tend to provide more conservative results. The use of train management data could be regarded as intermediate step between wayside monitoring (which is the reference) and the use of Eurocode fatigue load models.

Probabilistic fatigue evaluations have shown that updating of the uncertainty of influence lines using monitoring data contributed significantly to improving the result accuracy, as compared to the case with no prior information, in which model uncertainties according to recommendations of the probabilistic model code were used.

The updating of the numerical model provided a further increase of estimated reliability indices, at a cost of significant computational effort required to perform the model updating.

The results presented in this use case cannot be generalized. The increase of reliability index due to more accurate models of traffic loads and the numerical model of the bridge depend on many factors that are specific to the respective track section, the bridge structure and the monitoring system applied.

The purpose of this work was rather to present an approach that encompasses dealing with uncertainties on the side of traffic loads as well as of the structural response, and joins them together with probabilistic definition of fatigue resistance in a full-probabilistic evaluation of the fatigue reliability index.

The application of the presented methods could be recommended especially for cases where larger discrepancies between the original fatigue assessment assumptions and the reality are suspected. This may apply to bridges on track sections with much lower (or much higher) portion of freight traffic, or sections where freight trains operate with a significant number of empty wagons. Further, bridges with larger modelling uncertainties may profit from the use of monitoring data, for example short bridges (due to uncertain track interaction) or bridges that were calculated using models with significant simplifications, especially simplifications of member connections.

ACKNOWLEDGMENTS

This work was done within the scope of the Shift2Rail project Assets4Rail (Grant agreement no: 826250) funded by the European Commission.

REFERENCES

[1] A. Dinas, Th.N. Nikolaidis, C.C. Baniotopoulos: Sustainable Restoration Criteria for a Historical Steel Railway Bridge, Procedia Environmental Sciences vol. 38, p. 578-585, 2017.

[2] G. Zhang, Y. Liu, J. Liu, S. Lan, J. Yang: Causes and statistical characteristics of bridge failures: A review, Journal of. Traffic and Transportation Engineering (engl. ed.) vol. 9, p. 388-406, 2022.

[3] X.W. Ye, Y.Q. Ni, K.Y. Wong, J.M. Ko: Statistical analysis of stress spectra for fatigue life assessment of steel bridges with structural health monitoring data, Engineering Structures vol. 45, p. 166-176, 2012.

[4] J. Leandera, A. Anderssona, R. Karoumi: Monitoring and enhanced fatigue evaluation of a steel railway bridge, Engineering Structures vol. 32, p.854-863, 2010.

[5] S.E. Azam, M.M. Didyk, D. Linzell, A. Rageh: Experimental validation and numerical investigation of virtual strain sensing methods for steel railway bridges, Journal of Sound and Vibration vol. 537, 117207, 2022.

[6] K. Maes, G. Lombaert: Validation of virtual sensing for the reconstruction of stresses in a railway bridge using field data of the KW51 bridge, Mechanical Systems and Signal Processing vol. 190, 110142, 2023.

[7] R. Teixeira, C.S. Horas, A.M.P. De Jesus, R. Calçada, T.N. Bittencourt: Innovative hierarchical fatigue analysis of critical riveted railway bridges: A case study, Engineering Structures vol. 317, 118629, 2024.

[8] G.T. Frøseth, A. Rönnquist: Load model of historic traffic for fatigue life estimation of Norwegian railway bridges, Engineering Structures vol. 200, 109626, 2019.

CC BY 4.0
https://creativecommons.org/licenses/by/4.0/deed.en
This CC license does not apply to third party material and content noted otherwise

DOI: 10.3217/978-3-99161-057-1-008

[9] S. Verdenius, S. Hengeveld, J. Maljaars: New fatigue load models for assessing railway bridges in Europe, Engineering Structures vol. 284, 115914, 2023.
[10] M. Ralbovsky, A. Vorwagner, S. Lachinger: History of rail traffic volumes in the evaluation of fatigue consumption in steel bridges, 5th International Conference on Railway Technology, Montpellier, France, 22.-25.8.2022
[11] C.S. Horas, J.N. Silva, J.A.F.O. Correia, A.M.P. De Jesus: Fatigue damage assessment on aging riveted metallic railway bridges: A literature review, Structures vol.58, 105664. 2023.
[12] Y.H. Su, X.W. Ye, Y. Ding: ESS-based probabilistic fatigue life assessment of steel bridges: Methodology, numerical simulation and application, Engineering Structures vol. 253, 113802, 2022.
[13] S. Lachinger, M. Ralbovsky, A. Anžlin, M. Kosič: project Assets4Rail - H2020 Shift2Rail ERJU grant 826250 - Deliverable D3.4: Fatigue consumption and remaining lifetime of structural components, 2022.
[14] SALOME, 2019 v 9.4. [Online]. Available: www.salome-platform.org
[15] G. Dhondt: Calculix v 2.16. [Online]. Available: www.calculix.de
[16] A. Anžlin, M. Ralbovsky, D. Hekič, J. Kalin, M. Kreslin: project Assets4Rail - H2020 Shift2Rail ERJU grant 826250 - Deliverable D3.2: Section-specific fatigue load models: method and application, 2021.
[17] Joint Comitee on Structural Safety, JCSS Probabilistic Model Code; Parts I - IV, JCSS, 2001-2015

CC BY 4.0
https://creativecommons.org/licenses/by/4.0/deed.en
This CC license does not apply to third party material and content noted otherwise